**To cite this version :**

# Thermal significance and optimal transfer in vessels bundles is influenced by vascular density

J. Dichamp [a], F. De Gournay [b], F. Plouraboué [a,*]

[a] *Institut de Mécanique des Fluides de Toulouse, UMR CNRS-INPT/UPS No. 5502, France*
[b] *Institut de Mathématiques de Toulouse, CNRS and Université Paul Sabatier, Toulouse, France*

ABSTRACT

A semi analytic method is used in order to systematically compute stationary 3 D coupled convection diffusion in various parallel counter current configurations and evaluate their thermal significance. This semi analytic method permits a complete exploration of physiologically relevant parameter space associated with the bio heat transfer of parallel vessels bundles. We analyze thermal significance with various previously proposed criteria. Optimal transfer configurations are found to depend on the vascular density and Péclet numbers. The relevance of these findings for bio heat modeling in tissues is discussed.

## 1. Introduction

Bio heat transfer is relevant in many physiological contexts such as thermoregulation, lypolysis, or thermo therapies among others. On the contrary to most heterogeneous medium, biological tissues are living dynamic structures. They experience both local convection inside vessels, diffusion in complex structures in addition with reaction rates inside tissue. The complexity of micro vasculature is a serious hindrance for exhaustively taking into account the role of the vascular exchanges in bio heat transfer. This is why various models have been proposed to approximately describe bio heat exchanges [1 5]. This is especially true for convection within parallel vessels, the relevance of which can be found in many physiological contexts (e.g. muscles, bones, etc...) [6 9]. Quoting [9], 'since a considerable fraction of blood vessels are found in pairs vessel vessel heat transfer has generally been postulated as one of the most important heat transfer mechanisms involved in determining the tissue temperature distributions' [10 12]. This is why the case of parallel vessels bundles has received some attention [9,6 8].

In a broader context heat transfer in tube bundles has also been previously investigated in the search for optimal transfer configurations. For natural convection [13] found interesting scaling laws for optimal spacing between tubes. Furthermore, when some external forced flows is applied around the tube bundles (considered has solid sources) a rather important body of literature can be found, e.g. [14,15]. Other more complex configuration for optimal transfer has also been investigated such as trees [16] or for pulsated flows in tubes [17].

An alternative approach to address and simplify heat transfer in tissue, is to realize that not every vessel participates to heat exchanges. This is indeed known that, from convection dominated arterial inlets, when progressing down into the vascular three, the heat flux (vessel to tissue) gradually shrinks downward so as to reach equilibrium with the surrounding tissue. This simplified picture, might not exactly turn out to be true is some extreme case, when the metabolic production and/or consumption inside the tissue produces temperature gradients associated with 'hot' heat sources or sinks. However, we will see in the following that, in most physiologically relevant situations, heat production/consumption from the tissue metabolism has a negligible influence on heat fluxes. Hence, in most tissue heat transfer is mostly geometrically (e.g., related to the size, shape, length and distances between vessels) and thermally (e.g., associated with the inlet, outlet and relative blood flows) controlled. In this context, it is interesting to be able to know, a priory, when a vessel will mainly equilibrate its heat exchanges with the surrounding tissue so as to be able to infer, which vessels are thermally significant.

Thermal significance, has been discussed quite abundantly in the literature [18,4,19 23]. Since, generically, the local transfer

* Corresponding author.
  *E-mail addresses:* jules.dichamp@imft.fr (J. Dichamp), frederic.de-gournay@insa-toulouse.fr (F. De Gournay), franck.plouraboue@imft.fr (F. Plouraboué).

rate from the fluid into the solid is found to abruptly decay from the inlet along the longitudinal direction [24,25], it has been considered that some exponential decay with typical decaying length provide the typical length associated with thermal relaxation. This phenomenological choice is indeed justified in the case of parallel tube exchangers for which it is proven that generalized Graetz decomposition with an infinite set of exponentially decaying modes in the longitudinal direction holds [26–30]. Since thermal significance has also been investigated with other criteria than relaxation length, i. e arterial efficiency (Cf Section 2.4) we wish to analyze and compare them so as to get a more comprehensive analysis of the interest and validity of thermal significance.

Hence, in this paper, we analyze various distinct features of heat transfer in vessels bundles, associated with thermal significance, and optimal transfer using a quasi analytic approach previously described in [29,30]. In Section 2 the set of governing equations and their dimensionless formulation are provided. Some insights about the parameters used and their physiological relevance is discussed in Section 2.4. In Section 3 we first analyze unbalanced counter current configuration for transfer. We first investigate the influence of vessels radius in Section 3.1 so as to show that, when vessels are few diameter apart, this parameter is intrinsically irrelevant, being mainly taken care of by Péclet numbers ratio. Then, we pursue the analysis of thermal significance through the analysis of arterial effectiveness in Section 3.2 as well as thermal equilibrium length in Section 3.3 versus relevant dimensionless parameters. Finally we analyze heat transfer in Section 3.4 for which optimal configurations are brought to the fore.

## 2. Governing problem and dimensionless formulation

### 2.1. Configuration under study

In this paper we wish to analyze the vessel/tissue transfer in idealized bundles of parallel vessels, as depicted in Figs. 1 and 2. The tissue/vessel system is modeled as a transversely infinite exchanger into which a pattern of periodic parallel vessels transport heat. This choice has been made so as to gain insight into the exchanges independently of the transverse boundary conditions as opposed to [30]. To be more precise on the terminology that we will use in the following we will refer to the exchanger region as the finite (but transversely periodic) domain within

$[0, L_s] \times [0, L_s] \times [0, L_e]$ depicted in Fig. 1. Hence, the tissue model under study has a finite extent in the longitudinal direction, but needs boundary conditions for the heat at tubes inlets and outlets. In order to circumvent the problem of arbitrarily setting such boundary conditions at $z \equiv 0$ and $z \equiv L_e$, we connect the finite tissue exchanger to infinite inlet and outlet reservoirs connecting tubes, as in [28,30]. Hence three compartments are considered. The inlets and outlets where convection diffusion arises in the vessels only, and the tissue exchanger.

As in [30], we consider laminar convection diffusion arising in a fluid having constant properties. In the following we consider tubular vessels having circular sections. The artery is considered as the hot reference whilst the vein outlet provide the cold one (most results hereby presented do not depend on this arbitrary choice). Fully developed Poiseuille longitudinal velocity is prescribed in each vessels $\mathbf{v}_a \equiv v_a(r)\mathbf{e}_z \equiv 2V_a\left(1 - (r/R_a)^2\right)\mathbf{e}_z$ and $\mathbf{v}_v \equiv v_v(r)\mathbf{e}_z \equiv 2V_v\left(1 - (r/R_v)^2\right)\mathbf{e}_z$ where $V_a$ — respectively $V_v$ — and $R_a$ — respectively $R_v$ — stands for the average velocity and radius of the artery — respectively vein — and $\mathbf{e}_z$ is the unit vector along $z$ direction. The 'hot' arterial vessel refers to the tube with homogeneous inlet temperature at plus infinity $T_a^{+\infty}$ and the 'cold' vessel tube refers to the tube with homogeneous inlet temperature at minus infinity $T_v^{-\infty}$ as represented on Fig. 1.

In most of the following we will consider unbalanced counter current configuration where longitudinal velocities are different such that $V_a \geqslant V_v$ since this is mostly what arises in most physiological contexts. In this work we investigate three family of geometrical parameters: the arterial and vein radius, their length and their distances. Keeping with dimensionless geometrical parameters this leads to radius ratio $R^\star \equiv R_v/R_a$, vessel's aspect ratio $L^\star \equiv L_e/R_a$ and the dimensionless distance between vessels $\alpha^\star \equiv R_a/R_0$. In the chosen configuration associated with periodic bundles of vessels, the last parameter is directly related with the vessels surface density also equals to the volumic vascular density, i.e. vessel's volume over total volume, denoted $\phi \equiv \frac{4\pi R^{\star 2}}{L_s^{\star 2}}$ (note that this volumic vascular density also equals the transverse surfacic vascular density, since the hereby considered configuration is invariant along $z$ direction). The relation between $\phi$ & $\alpha^\star$ reads $\phi(\alpha^\star) \equiv \frac{\pi\alpha^{\star 2}}{2}$ and is represented in Fig. 2.
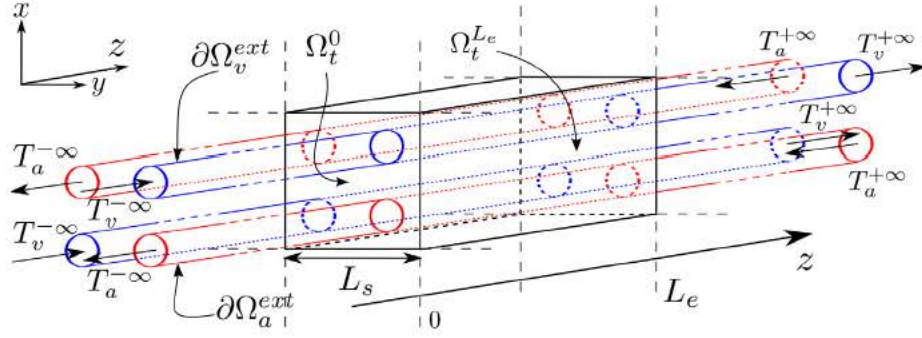
**Fig. 1.** Schematic layout of the elementary tissue geometry unit defining the tissue perfused by vessels bundles and the various important parameters associated with it: $L_e$ is the tissue/exchanger length, whilst $L_s$ is its period in transverse directions, both $x$ and $y$. $\Omega_t^0$, $\Omega_t^{L_e}$ denote the tissues sectional areas on exchanger's edges respectively on $z = 0$ and $z = L_e$. $\partial\Omega_a^{ext}$ and $\partial\Omega_v^{ext}$ denote the vessels sectional area outside the exchanger, i.e. within $z \in [-\infty, 0] \cup [L_e, +\infty]$. $T_a^{+\infty}$ and $T_v^{+\infty}$ are the temperature imposed in some 'far field' reservoir in arteries and veins. $T_a^{-\infty}$ and $T_v^{+\infty}$ are the temperature resulting (and thus numerically evaluated) from the exchange inside the tissue/exchanger and are not specified.
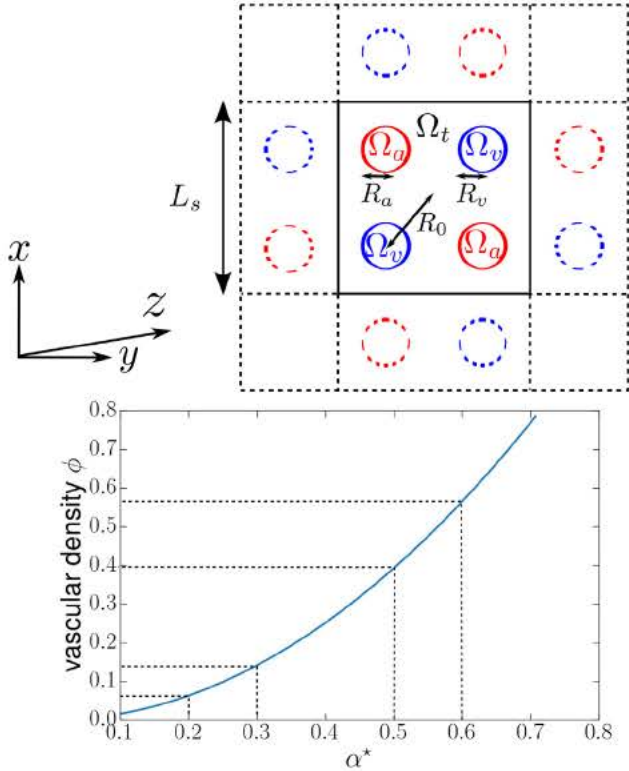


**Fig. 2.** Schematic layout of the transverse section of the tissue with periodic bundle of vessels. $R_a$ and $R_v$ are the arterial and venous radius, $R_0$ is the center-to-center distance between vessels and tissue. $\Omega_a$ stands for the arterial, $\Omega_v$ for the vein and $\Omega_t$ for tissue domain's sectional area inside the tissue exchanger. $L_s$ is the period of the transverse domain in both $x$ and $y$ directions. The graph below shows the relation between transverse normalized distance $\alpha$ and the vascular density $\phi = \pi\alpha^{\star 2}/2$.

## 2.2. Governing problem

Then, we write the stationary thermal energy balance in three dimensions as

$$\rho c \mathbf{v} \cdot \nabla T - k^F \Delta T = 0 \quad \text{in vessels}$$
$$k^T \Delta T = P \quad \text{in solid} \tag{1}$$

with $k^F$ being the fluid conductivity, $k^T$ the tissue one, $\rho$ the fluid density, $c$ the heat capacity and $P$ the metabolic heat production

inside the tissue [9]. The above problem reads more explicitly for longitudinally invariant velocity convection $\mathbf{v} = v(x,y)\mathbf{e}_z$,

$$\rho c\, v(x,y)\partial_z T - k^F\left(\partial_x^2 + \partial_y^2 + \partial_z^2\right)T = 0 \quad \text{in vessels}$$
$$k^T\left(\partial_x^2 + \partial_y^2 + \partial_z^2\right)T = P \quad \text{in solid} \tag{2}$$

Then continuity of temperature and fluxes at vessels/tissue interfaces $\partial\Omega_a$ (for artery surface) and $\partial\Omega_v$ (for vein surface), that we note here $\partial\Omega_{a,v}$ read as

$$T|_{\partial\Omega_{a,v}} = T|_{\partial\Omega_t}$$
$$k^F\partial_n T|_{\partial\Omega_{a,v}} = k^T\partial_n T|_{\partial\Omega_t} \tag{3}$$

On the external part of the exchanger configuration, i.e. for $z \leqslant 0$ or $z \geqslant L_e$ we consider homogeneous Neumann conditions as in [30]

$$\partial_n T|_{\partial\Omega_{a,v}^{ext}} = 0 \tag{4}$$

For the edges of the tissue domain on $z = 0$ and $z = Le$ we consider homogeneous adiabatic Neumann conditions,

$$\partial_n T|_{\partial\Omega_t^{0,Le}} = 0 \tag{5}$$

At infinity, in the artery tube section $\Omega_a$ and in the vein section $\Omega_v$, temperatures are imposed

$$T|_{\Omega_a}(x,y,z \to +\infty) = T_a^{+\infty}$$
$$T|_{\Omega_v}(x,y,z \to -\infty) = T_v^{-\infty}, \tag{6}$$

## 2.3. Dimensionless formulation

Following previous studies (e.g. [31]), let us now use dimensionless variable with $\star$ index defined as $x = R_a x^\star, y = R_a y^\star$, $z = R_a z^\star, L_e = L^\star R_a, v_a = 2V_a v_a^\star, v_v = 2V_v v_v^\star$, and

$$T^\star = \frac{T - T_a^{+\infty}}{T_a^{+\infty} - T_v^{-\infty}} + \frac{T - T_v^{-\infty}}{T_a^{+\infty} - T_v^{-\infty}}. \tag{7}$$

Now, using the dimensionless position $\xi^\star = (x^\star, y^\star)$ in the $(x,y)$ plane (2) now reads

$$Pe_{a,v} v^\star(\xi^\star)\partial_{z^\star}T^\star - \left(\partial_{x^\star}^2 + \partial_{y^\star}^2 + \partial_{z^\star}^2\right)T^\star = 0, \quad \text{in Vessels}$$
$$\left(\partial_{x^\star}^2 + \partial_{y^\star}^2 + \partial_{z^\star}^2\right)T^\star = P^\star, \text{in Tissue} \tag{8}$$

with, Péclet number being $Pe_{a,v} = 2\rho c V_{a,v} R_{a,v}/k^F$, and dimensionless metabolic source term

$$P^\star \quad \frac{PR^2}{k_t\left(T_a^{+\infty} \quad T_v^{-\infty}\right)}. \tag{9}$$

At the interface between vessels $\partial\Omega_v$ and tissue edge $\partial\Omega_t$ inside the exchangers one has continuity of temperature and fluxes

$$
\begin{aligned}
T^\star|_{\partial\Omega_{a,v}^\star} \quad & T^\star|_{\partial\Omega_t^\star} \\
k^F\partial_n T^\star|_{\partial\Omega_{a,v}^\star} \quad & k^T\partial_n T^\star|_{\partial\Omega_t^\star}.
\end{aligned}
\tag{10}
$$

Due to the choice of dimensionless temperature the imposed cold and hot sources verify

$$
\begin{aligned}
T^\star|_{\Omega_a^\star}(\xi^\star, z^\star \to +\infty) \quad T_a^{\star+\infty} \quad 1 \quad \text{in arterial inlet} \\
T^\star|_{\Omega_v^\star}(\xi^\star, z^\star \to \quad\infty) \quad T_v^{\star\quad\infty} \quad 1 \quad \text{in venous inlet}
\end{aligned}
\tag{11}
$$

## 2.4. Dimensionless parameters and thermally significant numbers

Dimensionless formulation thus brings seven different dimensionless parameters: two hot and cold Péclet numbers $Pe_{a,v} \quad 2\rho c V_{a,v} R_{a,v}/k^F$, the conductivity ratio between the tissue and the blood $k^T/k^F$, vessels aspect ratio $L^\star \quad L_e/R_a$, vessels radius ratio $R^\star \quad R_v/R_a$, dimensionless distance $\alpha^\star \quad R_a/R_0$ and finally the dimensionless metabolic rate $P^\star \quad PR^2/k_t(T_a^{+\infty} \quad T_v^{-\infty})$. In order to more closely delimit physiologically relevant parameter space, we prescribe a conductivity ratio $k^T/k^F \quad 1$, since it is generally very close to one in most tissues [32]. Furthermore, using data obtained from [9] for muscle where $k_t \quad 0.5$ W K $^1$ m $^1$, $R \quad 500$ μm, $T_a^{+\infty} \quad 37$ °C, assuming outlet venous temperature $T_v^{+\infty} \quad 35$ °C, as well as $P \quad 675$ W m $^3$ for hypothermia and $P \quad 97000$ W m $^3$ for hyperthermia, we found the following range: $P^\star$ $1.7 \; 10^{-4} \quad 2.4 \; 10^{-2}$.

Hence, in the following we neglect the influence of the metabolic source term $P^\star$. The significant parameter space dimension is thus five, rather than seven, associated with $Pe_a, Pe_v, L^\star, \alpha^\star$ and $R^\star$. Hence, we mainly focus our interest toward physiologically relevant parameters for which $Pe_v$ is fixed at various value between 5 to 20, whilst varying $Pe_a$ between 5 to several hundreds. We explore the effect of $L^\star, \alpha^\star$ and $R^\star$ on the vessels thermally significance as well as heat transfer.

Three additional dimensionless parameter of interest are also resulting from the considered configuration for evaluation of thermal significance. Let us first define spatial averaging (more precisely dimensionless surface averaging) using notation $\overline{T}_i \quad \int_{\Omega_i} T d\Omega_i / \int_{\Omega_i} d\Omega_i$, with index $i \quad a, v, t$ respectively associated with $\Omega_a$ the arterial, $\Omega_v$ venous and $\Omega_t$ tissue domain's transverse sections, as depicted in Fig. 2. Then, the arterial efficiency $\epsilon_a$ has been defined and used [18,4,19 21],

$$
\epsilon_a \quad \frac{\overline{T_a}^\star(z^\star \; 0) \quad \overline{T_t}^\star(z^\star \; 0)}{\frac{T_a^{\star,+\infty} \quad T_v^{\star,\quad\infty}}{\quad} \quad \frac{\overline{T_a}^\star(z^\star \; 0) \quad \overline{T_t}^\star(z^\star \; 0)}{2}}
\tag{12}
$$

Secondly, thermal significance has also been related to the exponential decay of the temperature along vessels [22,23] through the vessels thermal equilibrium length $\ell_{eq}^\star$. It is here defined as the length for which the average temperature decays by an exponential factor from the arterial entrance (here in $z^\star \quad L^\star$)

$$\overline{T_t}^\star\left(\ell_{eq}^\star\right) \quad \left(1 \quad e^{-1}\right)\overline{T_t}^\star(L^\star). \tag{13}$$

For this parameter to be independent of longitudinal length it must be expressed as a fraction of the exchanger's length, we will thus consider the ratio $\ell_{eq}^\star/L^\star$

Thirdly, we consider the vessel's surface heat flux through the Nusselt number derived from dimensionless formulation as in [30]

$$Nu_{a,v} \quad 2\int_0^{L^\star} dz^\star \int_{\partial\Omega_{a,v}} \partial_{n^\star} T^\star d\Omega_{a,v} \tag{14}$$

where $\partial\Omega_{a,v}$ is the edge of arterial and vein (which are circles) and $d\partial\Omega_{a,v}$ is the integration element along those edges.

### 2.4.1. Biological relevance of the parameter choices

Since most studies related to bioheat do not consider dimensionless numbers, it is interesting to evaluate values arterial and venous Péclet on different physiological contexts. Table 1 provides these figures evaluated from thermal measurements performed on two species in different organs. Péclet values range from 0.23 to 263.66 for the arterial part of the circulation and from 0.07 to 118.68 for the venous one. Typical ratio between arterial and venous range from 2.22 to 3.29. In most of the results presented in forthcoming sections, we considered venous Péclet $Pe_v \quad 5$ and 10 associated with the small/intermediate part of the circulation. This choice is also motivated by trying to infer the influence of venous Péclet on other parameters by doubling its value. Furthermore, the arterial to venous Péclet range is chosen between 1 to 20. This is higher than in the reported values of Table 1 but one has to born in mind that these measurements are obviously limited, and do not cover the entire range of physiologically relevant situations (e.g. arterioles and arteries vasodilate so as to increase blood flow leading to higher Péclet ratios). In any case, studying the limit of high Péclet ratio is interesting to understand the asymptotic behavior of vascular bundles.

Finally it is interesting to mention that vessels density $\phi$ in most tissues rarely reach values larger than 20%, except for special contexts. Nevertheless, it can be locally very large in the proximity of arterial and venule pairs. For being able to describe both generic situations and special cases, the values chosen for $\phi$ and $\alpha$ are illustrated Fig. 2.

## 2.5. General comments on the formulation and numerical method

The details of the numerical method used in this contribution has already been detailed in [28], as well as briefly described and used in [30]. [30] also provides several numerical validations of the method. The main idea of the numerical approach is to separate the whole problem into three distinct Graetz problems respectively associated with inlet tubes, outlet tubes and the exchanger (containing both tissue and fluid domains). Each Graetz problem follows a different expression of the dimensionless temperature field since there is a different spectral decomposition. The amplitudes of Graetz are then coupled together into a linear system which is set so as to 'match' the continuity of temperature and fluxes at the exchanger inlets and outlets. A detailed description of the method can be found in [28]. Let us just recall the theoretical

**Table 1**
Physiological values used for Péclet computation assuming that $c \quad 3651$ J/(kg·°C), $k^F \quad 0.51$ W/(m·°C) and $\rho \quad 1046$ kg/m³ [32].

| Physiological context | $D$(μm) | $V$ (mm/s) | $Pe$ |
|---|---|---|---|
| Human retina (venous bifurcations) [33] | 125.9 ± 26.44 | 8.63 ± 2.33 | 8.5 ± 3.81 |
| Dog mesenteric [34] | | | |
|   Main venous branches | 2511.89 | 6.31 | 118.68 |
|   Terminal veins | 1445.44 | 5.58 | 60.4 |
|   Venules | 32.11 | 0.29 | 0.07 |
|   Main artery branches | 1063.33 | 33.11 | 263.66 |
|   Terminal branches | 611.88 | 35.21 | 161.33 |
|   Arterioles | 22.22 | 1.36 | 0.23 |

expressions of the dimensionless temperature fields in each domain. For sake of simplicity we will just write the expressions for one arterial and one venous domains although there are four of each in our configuration.

$$T^\star(\xi^\star, z^\star) \quad \sum_{N^\star} x_n^+ T_n^+(\xi^\star) e^{\lambda_n^+ z^\star} + x_n T_n(\xi^\star) e^{\lambda_n(z^\star \ L^\star)} \quad z^\star \in [0, L^\star]$$

$$T^\star(\xi^\star, z^\star) \quad x_0^v + \sum_{N^\star} x_n^+ t_n^+(\xi^\star) e^{\mu_n^+(z^\star \ L^\star)} \quad \text{vein } z^\star \geqslant L^\star$$

$$T^\star(\xi^\star, z^\star) \quad x_0^a + \sum_{N^\star} x_n u_n(\xi^\star) e^{\gamma_n z^\star} \quad \text{artery } z^\star \leqslant 0$$

$$T^\star(\xi^\star, z^\star) \quad T_v^{\star \ \infty} + \sum_{N^\star} x_n t_n(\xi^\star) e^{\mu_n z^\star} \quad \text{vein } z^\star \leqslant 0$$

$$T^\star(\xi^\star, z^\star) \quad T_a^{\star+\infty} + \sum_{N^\star} x_n^+ u_n^+(\xi^\star) e^{\gamma_n^+(z^\star \ L^\star)} \quad \text{artery } z^\star \geqslant L^\star$$

$$(15)$$

with $x_n^\pm$ amplitudes of modes, $T_n^\pm, t_n^\pm$ and $u_n^\pm$ eigenvectors, $\lambda_n^\pm, \mu_n^\pm$ and $\gamma_n^\pm$ eigenvalues respectively of exchanger domain, venous domain and arterial domain.

As previously mentioned, dimensionless inlet temperatures $T_a^{\star+\infty}$ and $T_v^{\star \ \infty}$ values are respectively 1 et $\ $1 and unknowns $x_0^v, x_0^a$ are computed by the method as respectively the homo geneous temperature fields at minus infinity for the arterial vessels and plus infinity for the venous vessels.

# 3. Results

## 3.1. Influence of venous radius

Here, we first expose how vessel's radius influences heat trans fer. Fig. 3 provides the arterial transfer rate dependence versus the arterial to venous Péclet ratio $Pe_a/Pe_v$, whilst other parameters being prescribed. We investigate two different parameters that are fixed through change of radius variation. We first fix the venous Péclet number $Pe_v$ as compared to a reference simulation with $R_v^{\star ref} \quad R_v^{ref}/R_a \quad 1$ in Fig. 3a. We then fix, the flux ratio $Q^\star \equiv Q_v/Q_v^{ref} \quad (Pe_v R_v)/(Pe_v^{ref} R_v^{ref})$ is kept constant in Fig. 3b. In the later, a master curve for transfer is observed over a rather large range of Péclet ratio $Pe_a/Pe_v$, reaching a late plateau for large $Pe_a/Pe_v$ values, having a weak dependence on $R^\star$ (8% variations are observed in Fig. 3b when varying $R^\star$ by 100%). As expected, for a given vessel length aspect ratio $L^\star$, transfer effectiveness sat urates when increasing the arterial Péclet number, so as to reach a plateau for which there is no gain for transfer in increasing blood flow further. The value of this plateau is related to $L^\star$, but is also

related to the thermal equilibrium length $\ell_{eq}$ subsequently studied in Section 3.3. This observation indicates that the influence of $R^\star$ can be recast into the Péclet ratio $Pe_a/Pe_v$ variations, as long as $Q^\star$ is prescribed. Hence, one can reduce parameter space dimen sion by one, from fifth to four since the dependance with $R^\star$ is slave to a given value $Q^\star \equiv Q_v/Q_a \quad Pe_a/(Pe_v R^\star)$. We now further examine thermal significance and heat transfer effectiveness dependance with $Pe_a, Pe_v, \alpha^\star$ and $L^\star$.

## 3.2. Arterial effectiveness evaluation

Considering that average temperature is a figure of interest, the arterial effectiveness $\epsilon_a$ defined in (12) provides an estimate of the relaxation toward equilibrium between vessels and tissues. The greater $\epsilon_a$, the larger the exchanges, and the better thermal effec tiveness. Hence, similarly with the heat transfer performances, this average effectiveness $\epsilon_a$ monotonically levels off for increasing arterial convection. In Fig. 4, for fixed $Pe_v$, as $Pe_a$ increases over a wide range, $\epsilon_a$ grows toward a systematic saturation for highly convective transfer regime. Not surprisingly the precise value of venous Péclet number $Pe_v$ does not influence much the saturated values of $\epsilon_a$, since an uppermost gain of 20% is observed comparing Fig. 4a b for twice a value in $Pe_v$ (same comment applies to the comparison of Fig. 4c & d. This result can be explained by the fact that tissue/vessels exchanges are dominated by arterial/tissue fluxes rather than venous/tissues ones when the arterial Péclet $Pe_a$ is much larger than venous one (i.e. when $Pe_a/Pe_v \gg 1$). If true, this interpretation implies that, for almost equilibrated situations when $Pe_a/Pe_v$ is close to one, the precise value of $Pe_v$ should mat ter. This is confirmed by the observation that the corresponding $\epsilon_a$ almost doubles for twice a value in $Pe_v$ when $Pe_a/Pe_v \sim 1$ compar ing Fig. 4a b as well as Fig. 4c & d. Now considering the sensitivity of the arterial effectiveness $\epsilon_a$ to the vessels aspect ratio $L^\star$, one can note that when $L^\star$ is multiplied by four comparing Fig. 4a & c or similarly Fig. 4b & d, $\epsilon_a$ barely changes by more than 20% over the all range of Péclet ratio. It is interesting to note that, the unsen sitivity of $\epsilon_a$ to $L^\star$ drastically increases as $\alpha^\star$ augments. Indeed, in the most 'diluted' case, when $\alpha^\star \quad 0.2$, one can clearly observe a change between bullet curves of Fig. 4a & c. However, for larger values of $\alpha^\star$, changes in $\epsilon_a$ from Fig. 4a c and Fig. 4b d are very weak. This can be explained by the existence of heat transfer "screening length" associated with the transverse distance between vessels, given by dimensionless number $\alpha^\star$. As $\alpha^\star$ decreases, the transverse length between vessels becomes the pre dominant length scale for transfer, which 'screens' the influence of longitudinal length.
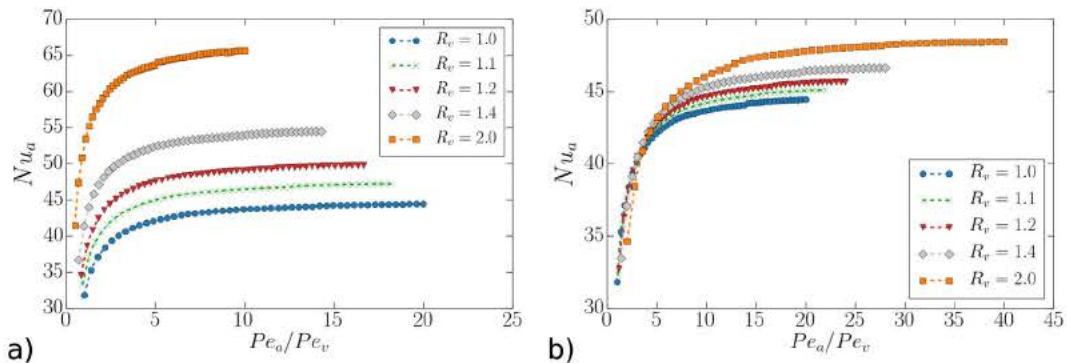


**Fig. 3.** Arterial Nusselt number versus Péclet ratio $Pe_a/Pe_v$ compared to reference simulation ($R^{ref} \quad R_a$, i.e. $R^\star \quad 1$) and $L^\star \quad 10, \alpha^\star \quad 0.2$, for (a) fixed venous Péclet ($Pe_v \quad Pe_v^{ref} \quad 10$), (b) fixed dimensionless venous flux $Q^\star \equiv Q_v/Q_v^{ref} \quad (Pe_v R_v)/(Pe_v^{ref} R_v^{ref})$ and $Pe_v^{ref} \quad 10$. For fixed dimensionless flux ratio $Q^\star$ in (b) a master curve is observed, especially at moderate Péclet ratio.
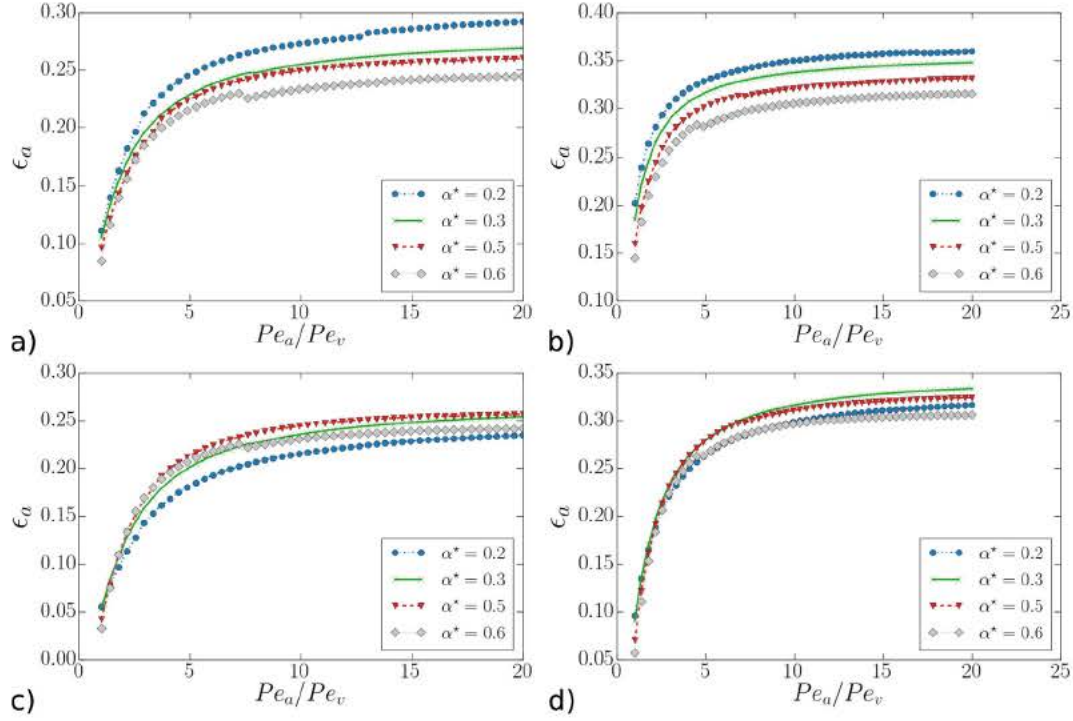
**Fig. 4.** Arterial effectiveness $\epsilon_a$ versus Péclet ratio $Pe_a/Pe_v$ for several distances between vessels $\alpha^\star = 0.2, 0.3, 0.5, 0.6$, venous Péclet $Pe_v$ and vessels aspect ratio $L^\star$ : (a) $Pe_v = 5, L^\star = 5$, (b) $Pe_v = 10, L^\star = 5$, (c) $Pe_v = 5, L^\star = 20$, (d) $Pe_v = 10, L^\star = 20$.
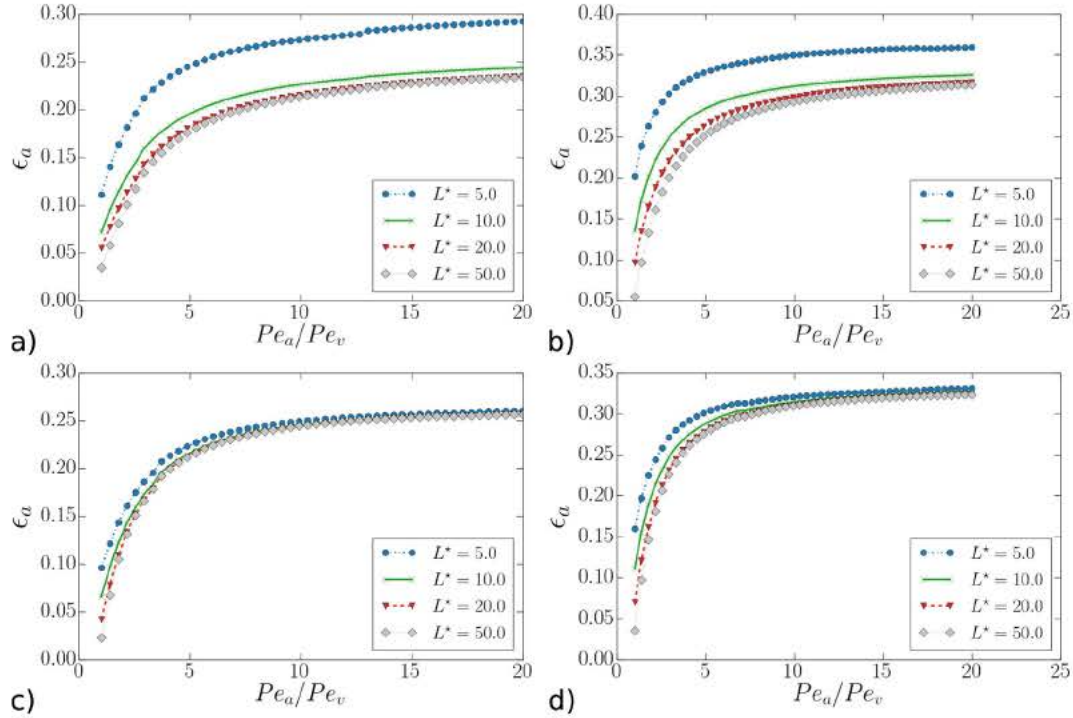


**Fig. 5.** Arterial effectiveness $\epsilon_a$ versus Péclet ratio $Pe_a/Pe_v$ for several vessels length $L^\star = 5, 10, 20, 50$, and several venous Péclet and distance between vessels: (a) $Pe_v = 5, \alpha = 0.2$, (b) $Pe_v = 10, \alpha = 0.2$, (c) $Pe_v = 5, \alpha = 0.5$, (d) $Pe_v = 10, \alpha = 0.5$.

This interpretation of the results of Fig. 4 are comforted by Fig. 5. When increasing $\alpha^\star$ from $\alpha^\star = 0.2$ in Fig. 5a & b to $\alpha^\star = 0.5$ in Fig. 5c & d, one can clearly see the unsensitivity of the arterial effectiveness $\epsilon_a$ to $L^\star$. We now wish to compare parameter sensitivity over the same range of parameters for the thermal equilibrium length $\ell_{eq}$.

### 3.3. Thermal equilibrium length evaluation

Effective equilibrium length (13) is evaluated in Fig. 6 over the same parameter range as in Fig. 4.

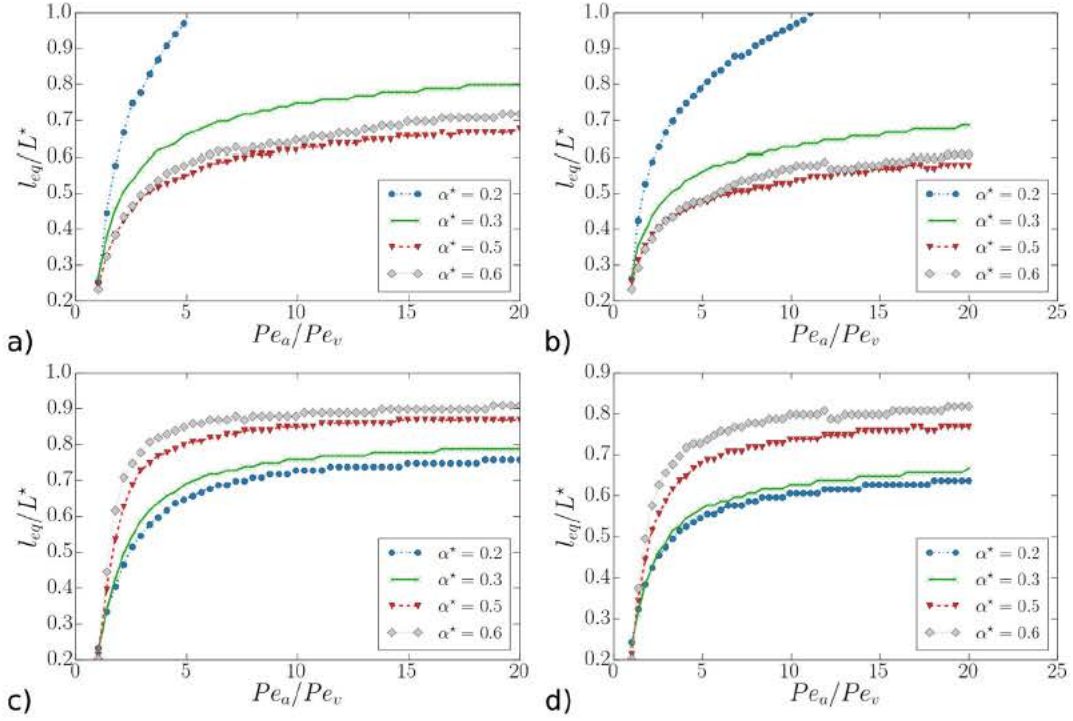A similar qualitative trend is found. For fixed venous Péclet number $Pe_v$, transfer effectiveness associated with $\ell_{eq}^\star/L^\star$ in Fig. 6

**Fig. 6.** Thermal equilibrium length ratio $\ell_{eq}/L^\star$ versus Péclet ratio $Pe_a/Pe_v$ for several distances between vessels $\alpha^\star$ 0.2, 0.3, 0.5, 0.6 and several venous Péclet $Pe_v$ and vessels length $L^\star$ : (a) $Pe_v$ 5, $L^\star$ 5, (b) $Pe_v$ 10, $L^\star$ 5, (c) $Pe_v$ 5, $L^\star$ 20, (d) $Pe_v$ 10, $L^\star$ 20.

increases with the arterial Péclet number $Pe_a$, so as to reach a plateau (obviously as long as $\ell_{eq}/L^\star < 1$). However, since $\ell_{eq}^\star/L^\star$ evaluates a dimensionless thermal balance length, the value of the plateau displays a clear dependance with both the transverse dimensionless distance between vessels, $\alpha^\star$, and vessel's aspect ratio $L^\star$. For moderate $L^\star$ in Fig. 6a & b, $\ell_{eq}^\star/L^\star$ first levels down as $\alpha^\star$ increases, then reaches a minimum and increases again. However, a different trend is found when $L^\star$ is larger (four times more) in Fig. 6c & d, so that the larger the transverse distance (i.e. the smaller $\alpha^\star$), the smaller $\ell_{eq}^\star/L^\star$. This observation is comforted, whilst presenting a slightly different shape in the results given in Fig. 7.

When increasing $\alpha^\star$ from $\alpha^\star$ 0.2 in Fig. 7a & b to $\alpha^\star$ 0.5 in Fig. 7c & d, the dependance with $L^\star$ of the dimensionless thermal equilibrium length $\ell_{eq}^\star/L^\star$ indeed differs. For small $\alpha^\star$ 0.2, i.e. large transverse distance between vessels (Fig. 7a & b)), $\ell_{eq}^\star/L^\star$ first levels down as $L^\star$ increases, so as to reach a minimal value, but increases again for large $L^\star$ value. This is due to the presence of a minimum in $L^\star$ as highlighted on figures Fig. 7c & d for a given Péclet ratio $Pe_a/Pe_v = 4$. On the contrary, for dense vessels bundles $\alpha^\star$ 0.5 (Fig. 7e & f), the thermal equilibrium length $\ell_{eq}^\star/L^\star$ monotonically increases with $L^\star$, i.e. the larger $L^\star$, the greater the ratio $\ell_{eq}^\star/L^\star$ so as to reach a plateau in the arterial convectively dominated regime. This observation indicates that when the longitudinal aspect ratio of vessels $L^\star$ is much greater than the dimensionless transverse typical distance $2/\alpha^\star$, then, the thermal equilibrium length is mainly controlled by $L^\star$ and increases with it.

Taking these results together, one can distinguish three different regimes: (i) either the vessels have large aspect ratio $L^\star$ and then the denser the bundle, the larger $\ell_{eq}^\star/L^\star$, (ii) either the vessel bundle is diluted and then the larger the aspect ratio, the larger $\ell_{eq}^\star/L^\star$, (iii) either both aspect ratio and vascular density are mod-

erate and a local sub optimum exists in term of $L^\star$ and $\alpha^\star$. Thermal equilibrium length ratio optimum is for example illustrated on Fig. 7c and d. Lastly, it can be noted on both Figs. 6 and 7 that the venous Péclet $Pe_v$ has a low influence on $\ell_{eq}^\star/L^\star$: doubling its value mostly results in a 20% variation of $\ell_{eq}^\star/L^\star$. As opposed to the arterial effectiveness study on previous section, this observation is true on every range of arterial to venous Péclets ratio $Pe_a/Pe_v$, even close to unity.

### 3.4. Arterial Nusselt evaluation

Let us now analyse the heat transfer in the same range of parameters as in the two previous sections. Fig. 8 presents the Nusselt number versus the arterial to venous Péclet number ratio. Depending on $\alpha^\star$ and $L^\star$, two regimes are observed: (i) for moderature value of $L^\star$, the Nusselt monotonically increases with $Pe_a$ (whatever $Pe_v$ value) towards reaching a plateau in the convectively dominated regime $Pe_a/Pe_v \gg 1$ (as for example found in [30]), (ii) for $L^\star \gg 1$ & $L^\star \gg 2/\alpha$, the Nusselt first increases with $Pe_a$, but after reaching a maximum, it gently decreases down.

The optimal Péclet ratio $Pe_a/Pe_v|_{opt}$ is mostly found moderate, whereas weakly depending on geometrical parameters. For example in Fig. 8d for $\alpha$ 0.5, $Pe_a/Pe_v|_{opt} \simeq 4$ whilst for $\alpha^\star$ 0.6, $Pe_a/Pe_v|_{opt} \simeq 3$. Furthermore, as expected, Fig. 8 shows that heat transfer is greater for tight vessel bundles (i.e. $\alpha^\star$ 0.5, 0.6). This results is expected since the transverse temperature gradient between veins and arteries are greater in this case.

Fig. 9 more clearly illustrates these two regimes and their dependance with $\alpha^\star$ and $L^\star$. The optimal Péclet ratio $Pe_a/Pe_v|_{opt}$ depends on $L^\star$, as can be seen when comparing Fig. 9a, b & c, where one can observe that, in the limit $L^\star \gg 1$, $Pe_a/Pe_v|_{opt}$ becomes closer and closer to unity. Also, the peak associated with the optimal value is much clearly identifiable in the $L^\star \gg 1$ limit. Again in
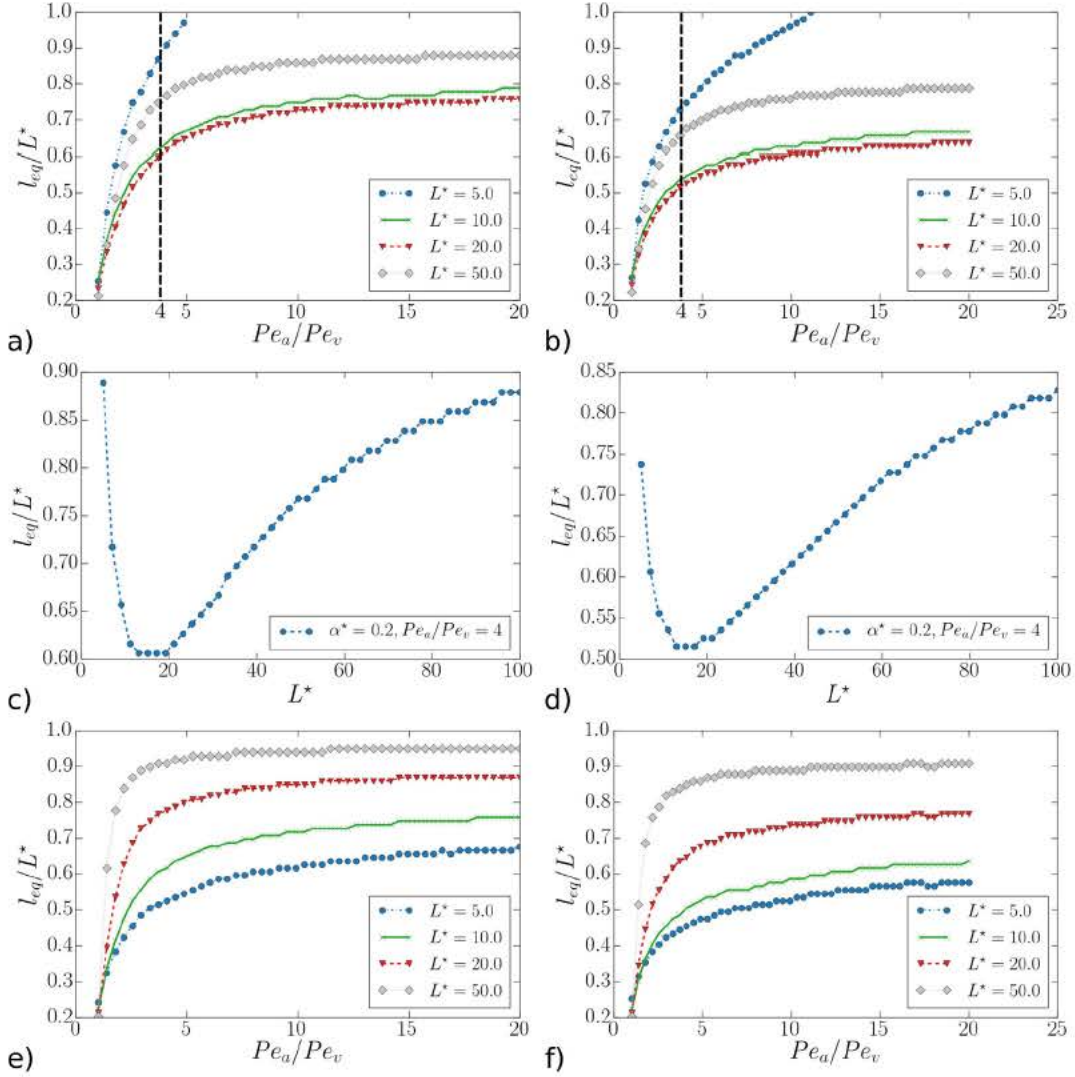
**Fig. 7.** Thermal equilibrium length ratio $\ell_{eq}^\star/L^\star$ versus Péclet ratio $Pe_a/Pe_v$ for several vessels length $L^\star$ 5, 10, 20, 50, and several venous Péclet and distance between vessels: (a) $Pe_v$ 5, $\alpha$ 0.2, (b) $Pe_v$ 10, $\alpha$ 0.2, (e) $Pe_v$ 5, $\alpha$ 0.5, (f) $Pe_v$ 10, $\alpha$ 0.5. (c) and (d) show $\ell_{eq}^\star/L^\star$ variations over $L^\star$ for $\alpha^\star$ 0.2 for respectively $Pe_v$ 5 and $Pe_v$ 10.

Fig. 9, one can see that the heat transfer is lower when vessels are far apart (i.e. for low $\alpha^\star$ values).

Now considering the influence of venous Péclet number, it can be similarly noted that doubling $\ell_{eq}/L^\star$ increases the arterial Nus selt alike. This is because the venous vessel drive thermal trans verse gradients thus increasing its Péclet number.

## 4. Discussion

The results presented in the previous section perform a system atic parametric exploration of thermally significance from two viewpoints. First, the 'averaged' viewpoint for which the arterial efficiency $\epsilon_a$ is evaluated. Secondly, a more local and physical view point associated with thermal equilibrium length. In both case, we found that thermal efficiency saturates when reaching the convectively dominated regime $Pe_a/Pe_v \gg 1$. These findings are consistent with the expectation that thermal exchanges are 'geo metrically' limited, so that, beyond the limit where $Pe_a/Pe_v \sim 8$, there is no further gain in increasing the flow for enhancing the exchanges.

Nevertheless, the dependance with vessel aspect ratio $L^\star$ and dimensionless transverse distance $2/\alpha^\star$ slightly differs between

both viewpoints. We found that for small distances between ves sels, i.e. when $2/\alpha^\star \leqslant 4$, the arterial efficiency $\epsilon_a$ very weakly depends on the vessel aspect ratio $L^\star$, whereas on the contrary, when $2/\alpha^\star \gg 1$, it does, being greater for moderate vessel aspect ratio $L^\star$. This result might be due to the fact that, for small distance between vessels, i.e. relatively tight vessels bundles, $L^\star \gg 2/\alpha^\star$ an homogenized limit is reached for an effective heat transfer to be reached. From this limit, the bundle behaves as a single 'average' tube into which the efficiency saturates with $L^\star$: there is no gain in efficiency when increasing vessel length further in this regime. Similar homogenized regime is found for thermal equilibrium length $\ell_{eq}^\star/L^\star$ which saturates toward a plateau value on the $Pe_a/Pe_v \gg 1$ limit for $L^\star \gg 2/\alpha^\star$ and dense bundles ($\alpha^\star \sim \sqrt{2}/2$). On the contrary, in the limit of 'dilute' vessels bundle, i.e. $\alpha \ll 1$, & $L^\star \leqslant 2/\alpha^\star$, we found a minimum value for $\ell_{eq}^\star/L^\star$ corresponding to a sub optimal exchange between vessels and tissue.

Now considering the transfer evaluated from Nusselt numbers, two regimes have been found: (i) in the case where vessels are suf ficiently far (more than four diameter apart), the Nusselt number monotonically but moderately increases with arterial Péclet num ber, so as to saturate as $Pe_a/Pe_v \gg 1$ (reminiscent of what has been
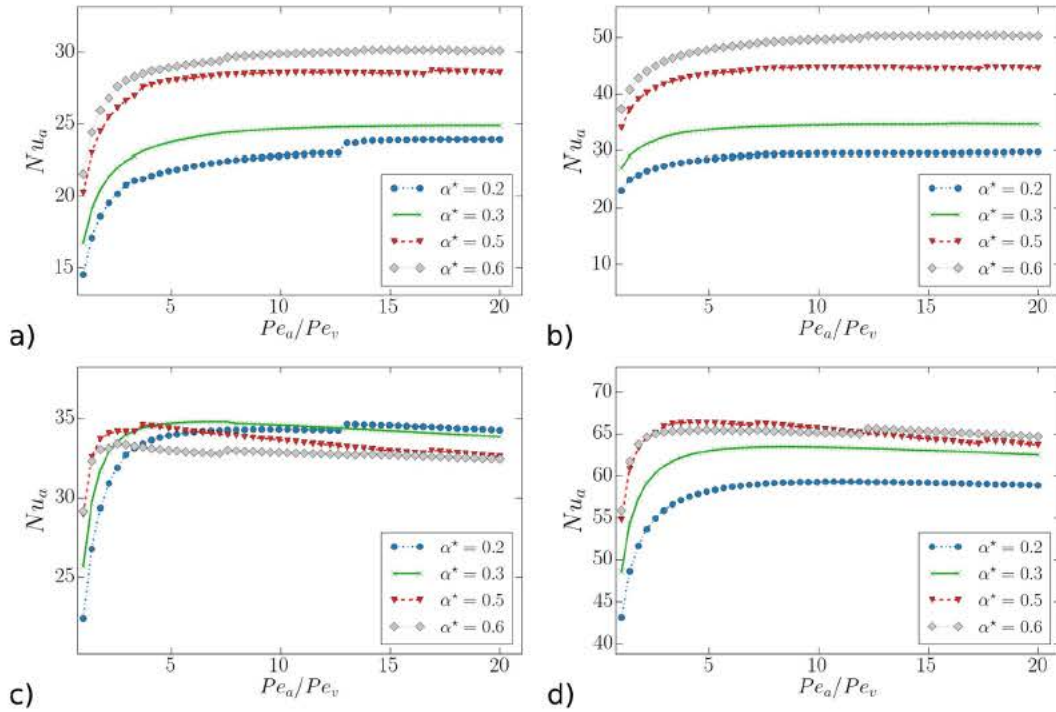
**Fig. 8.** Arterial Nusselt $Nu_a$ versus Péclet ratio $Pe_a/Pe_v$ for several distances between vessels $\alpha^\star$ 0.2, 0.3, 0.5, 0.6 and several venous Péclet $Pe_v$ and vessels length $L^\star$ : (a) $Pe_v$ 5, $L^\star$ 5, (b) $Pe_v$ 10, $L^\star$ 5, (c) $Pe_v$ 5, $L^\star$ 20, (d) $Pe_v$ 10, $L^\star$ 20.
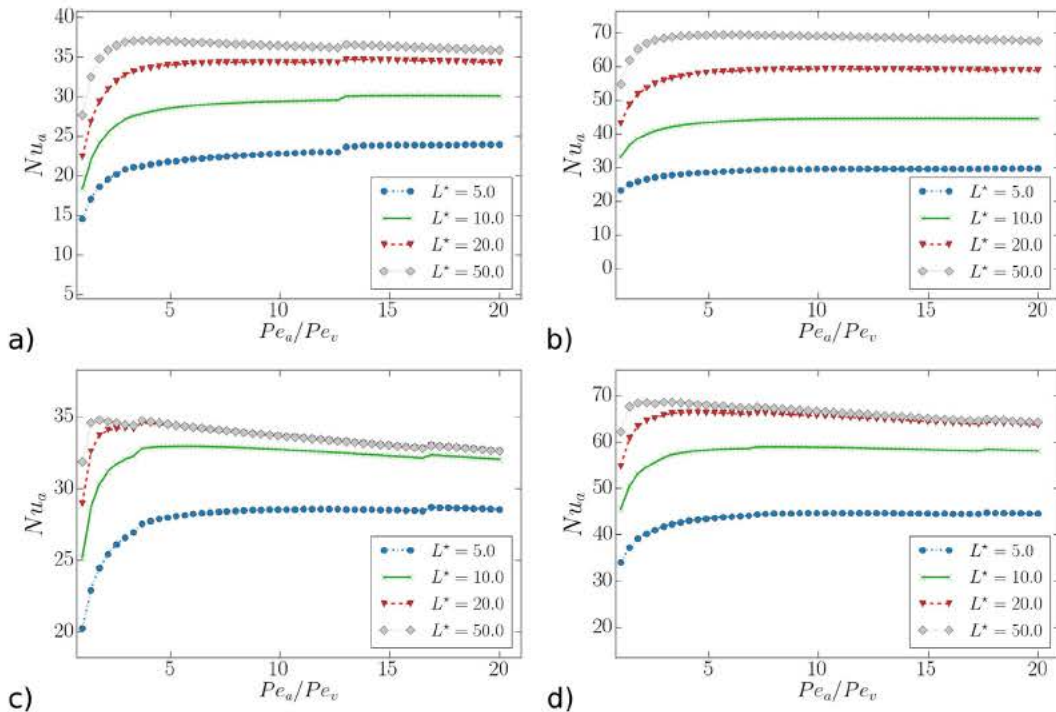


**Fig. 9.** Arterial Nusselt $Nu_a$ versus Péclet ratio $Pe_a/Pe_v$ for several vessels length $L^\star$ 5, 10, 20, 50, and several venous Péclet and distance between vessels: (a) $Pe_v$ 5, $\alpha$ 0.2, (b) $Pe_v$ 10, $\alpha$ 0.2, (c) $Pe_v$ 5, $\alpha$ 0.5, (d) $Pe_v$ 10, $\alpha$ 0.5.

found in [30]); (ii) in the opposite configuration of very closed vessels (less than two diameter apart), the Nusselt number display on optimal value for moderate Péclet number ratio only when the aspect ratio of the vessels are large enough ($L^\star \gg 2/\alpha^\star$). Nevertheless, in this second regime, the further decay of the heat echanges when increasing $Pe_a/Pe_v$ is quite weak, so that only ten to fifteen

percent of the optimal Nusselt value is lost when Péclet number ratio is set to ten time its optimal value. The physiological signifi cance of both regimes is interesting to discuss. The configuration associated with the first regime is relevant to many arterio venous pairs in muscles or bones, for which the Péclet number ratio is large. This regime shows that increasing the Péclet ratio

more than five time is useless for increasing heat transfer further. Hence, this regime specifies the range of 'physiological relevant' arterial and venous Péclet ratio for which the tissue is capable of heat regulation. The second regime is more relevant to dense cap illary beds for which the Péclet number ratio is more moderate. Obviously, the considered configuration is very idealised compared to real capillary beds. Nevertheless, this configuration shows that, in the relevant physiological range of parameters, i.e. $Pe_a/Pe_v$ within $[2 \quad 5]$, optimal transfer is indeed reached. This is consistent with the established fact that vessel/tissue exchanges are dominant at capillary scale.

## 5. Conclusions

This paper analyzes heat transfert in parallel tube bundles, for tissue heat transfer modelling. Considering a semi analytical approach using generalized Graetz mode decomposition, the effect of geometrical and thermal parameters is systematically investi gated in the relevant sets of dimensionless parameters. We found that the combination of both vascular density and aspect ratio of vessels influences markedly both thermal significance as well as transfer regimes.

## Declarations of interest

None.

## Acknowledgment

## References

[1] S. Weinbaum, L. Jiji, L. Lemons, Theory and experiment for the effect of vascular microstructure on surface tissue heat transfer – Part I: Anatomical foundation and model conceptualization, J. Biomech. Eng 106 (4) (1984) 321–330.

[2] S. Weinbaum, L.M. Jiji, A new simplified bioheat equation for the effect of blood flow on local average tissue temperature, J. Biomech. Eng 107 (2) (1985) 131–139.

[3] H.W. Huang, Z.P. Chen, R.B. Roemer, A Countercurrent vascular network model of heat transfer in tissues, J. Biomech. Eng 118 (1) (1996) 120–129.

[4] D.E. Lemons, S. Chien, L.I. Crawshaw, S. Weinbaum, L.M. Jiji, Significance of vessel size and type in vascular heat transfer, Am. J. Physiol.-Regul. Integr. Comp. Physiol. 253 (1) (1987) R128–R135.

[5] M. Zhu, S. Weinbaum, L.M. Jiji, Heat exchange between unequal countercurrent vessels asymmetrically embedded in a cylinder with surface convection, Int. J. Heat Mass Transf. 33 (10) (1990) 2275–2284.

[6] P. Yuan, Numerical analysis of an equivalent heat transfer coefficient in a porous model for simulating a biological tissue in a hyperthermia therapy, Int. J. Heat Mass Transf. 52 (7–8) (2009) 1734–1740.

[7] Y. Zhang, Generalized dual-phase lag bioheat equations based on nonequilibrium heat transfer in living biological tissues, Int. J. Heat Mass Transf. 52 (21–22) (2009) 4829–4834, https://doi.org/10.1016/j.ijheatmasstransfer.2009.06.007.

[8] A. Nakayama, F. Kuwahara, A general bioheat transfer model based on the theory of porous media, Int. J. Heat Mass Transf. 51 (11–12) (2008) 3190–3199, https://doi.org/10.1016/j.ijheatmasstransfer.2007.05.030.

[9] D. Shrivastava, R.B. Roemer, Readdressing the issue of thermally significant blood vessels using a countercurrent vessel network, J. Biomech. Eng 128 (2) (2006) 210–216. <http://www.ncbi.nlm.nih.gov/pubmed/16524332> .

[10] D.A. Pabst, S.A. Rommel, W.A. McLellan, T.M. Williams, T.K. Rowles, Thermoregulation of the intra-abdominal testes of the bottlenose dolphin (tursiops truncatus) during exercise, J. Exp. Biol. 198 (1) (1995) 221–226.

[11] J.W. Mitchell, G.E. Myers, An analytical model of the counter-current heat exchange phenomena, Biophys. J . 8 (8) (1968) 897–911.

[12] L. Zhu, Theoretical evaluation of contributions of heat conduction and countercurrent heat exchange in selective brain cooling in humans, Ann. Biomed. Eng. 28 (3) (2000) 269–277.

[13] A. Bejan, A.J. Fowler, G. Stanescu, The optimal spacing between horizontal cylinders in a fixed volume cooled by natural convection, Int. J. Heat Mass Transf. 38 (11) (1995) 2047–2055.

[14] M. Mon, U. Gross, Numerical study of fin-spacing effects in annular-finned tube heat exchangers, Int. J. Heat Mass Transf. 47 (8-9) (2004) 1953–1964.

[15] V. Mandhani, R. Chhabra, V. Eswaran, Forced convection heat transfer in tube banks in cross flow, Chem. Eng. Sci. 57 (3) (2002) 379–391.

[16] A. Bejan, M. Errera, Convective trees of fluid channels for volumetric cooling, Int. J. Heat Mass Transf. 43 (17) (2000) 3105–3118.

[17] L. Rocha, A. Bejan, Geometric optimization of periodic flow and heat transfer in a volume cooled by parallel tubes, J. Heat Trans.-T ASME 123 (2) (2001) 233–239.

[18] J.C. Chato, Heat transfer to blood vessels, J. Biomech. Eng 102 (1980) 331–341.

[19] H. Brinck, W.J. Werner., Estimation of the thermal effect of blood flow in a branching countercurrent network using a three-dimensional vascular model, J. Biomech. Eng 116 (1994) 331–341.

[20] Q. He, Experimental measurements of the temperature variation along artery-vein pairs from 200 to 1000 $\mu$m diameter in rat hind limb, J. Biomech. Eng 124 (6) (2002) 656–661.

[21] J.W. Baish, Formulation of a statistical model of heat transfer in perfused tissue, J. Biomech. Eng 116 (4) (1994) 521–527.

[22] M.M. Chen, K.R. Holmes, Microvascular contributions in tissue heat transfer, Ann. NY Acad. Sci. 335 (1980) 137–150.

[23] L. Zhu, D.E. Lemons, S. Weinbaum, Microvascular thermal equilibration in rat cremaster muscle, Ann. Biomed. Eng. 27 (1) (1996) 56–66.

[24] W. Escher, B. Michel, D. Poulikakos, A novel high performance, ultra thin heat sink for electronics, Int. J. Heat Fluid Flow 31 (4) (2010) 586–598.

[25] W. Qu, I. Mudawar, Experimental and numerical study of pressure drop and heat transfer in a single-phase micro-channel heat sink, Int. J. Heat Mass Transf. 45 (2002) 2549–2565.

[26] C. Pierre, F. Plouraboué, Numerical analysis of a new mixed-formulation for eigenvalue convection-diffusion problems, SIAM.J. Appl. Math 70 (2009) 658–676.

[27] J. Fehrenbach, F. De Gournay, C. Pierre, F. Plouraboué, The generalized Graetz problem in finite domains, SIAM. J. Appl. Math 72 (2012) 99–123.

[28] C. Pierre, J. Bouyssier, F. de Gournay, F. Plouraboué, Numerical computation of 3D heat transfer in complex parallel heat exchangers using generalized Graetz modes, J. Comp. Phys 268 (2014) 84–105.

[29] C. Pierre, J. Bouyssier, F. Plouraboué, Mathematical analysis of parallel convective exchangers, Math. Models Methods Appl. Sci. 24 (4) (2013) 627–667.

[30] J. Dichamp, F.D. Gournay, F. Plouraboué, Theoretical and numerical analysis of counter-flow parallel convective exchangers considering axial diffusion, Int. J. Heat Mass Transf. 107 (2017) 154–167.

[31] A.E. Quintero, M. Vera, B. Rivero-de Aguilar, Wall conduction effects in laminar counterflow parallel-plate heat exchangers, Int. J. Heat Mass Transf. 70 (1-3) (2014) 939–953.

[32] R.L. Mcintosh, V. Anderson, A comprehensive tissue properties database provided for the thermal assessment of a human at rest, Biophys. Rev. Lett. 5 (3) (2010) 129–151.

[33] R.M. Werkmeister, N. Dragostinoff, S. Palkovits, R. Told, A. Boltz, R.A. Leitgeb, M. Gröschl, G. Garhöfer, L. Schmetterer, Measurement of absolute blood flow velocity and blood flow in the human retina by dual-beam bidirectional Doppler Fourier-domain optical coherence tomography, Invest.e Ophthalmol. Visual Sci. 53 (10) (2012) 6062–6071, https://doi.org/10.1167/iovs.12-9514.

[34] T.W. Secomb, Hemodynamics, Comprehen. Physiol. 6 (2) (2016) 975–1003, https://doi.org/10.1002/cphy.c150038. <http://doi.wiley.com/10.1002/cphy.c150038> .